Dependence of the enantioselectivity on reversion of layer directions in cholamide inclusion compounds†

Kazuaki Aburaya, Ichiro Hisaki, Norimitsu Tohnai and Mikiji Miyata*

Received (in Cambridge, UK) 17th April 2007, Accepted 27th July 2007
First published as an Advance Article on the web 9th August 2007
DOI: 10.1039/b705822e

Cholamide includes 2,2-dimethyl-3-hexanol with high enantioselectivity, which is derived from reversion of layer direction due to a methyl group added to 2-methyl-3-hexanol.

Chiral recognition has received much attention from theoretical as well as practical viewpoints.[1] Crystalline lattice-type inclusion compounds provide detailed structural information for elucidation of chiral recognition mechanism. Enantioresolution of racemates such as alcohols,[2a,b] sulfoxides,[2c,d] lactones,[2e,f] and ketones,[2g] has been carried out using many artificial host compounds. However, enantioresolution of secondary aliphatic alcohols still remains a challenging problem.[3] The reason is that it is very difficult to recognize chirality, since the fourth substituent at the stereogenic carbon is the smallest atom, hydrogen, as shown in Fig. 1.

We previously reported that 3-epicholic and 3-epideoxycholic acids serve as excellent hosts for the enantioresolution of the alcohols due to CH/O interaction.[4] Although we also attempted to resolve some aliphatic secondary alcohols by cholamide (CAM) inclusion compounds, these included alcohols showed low enantioselectivity (less than 60% ee).[5] Recently, we have found another fascinating host–guest system in CAM inclusion compounds. Here we report preferable enantioresolution of 2,2-dimethyl-3-hexanol (**3**) for 2-methyl-3-hexanol (**2**) by CAM inclusion compounds. The high enantioselectivity comes from an additional methyl group which causes reversion of an arrangement of the host molecules to fix alkyl groups of the alcohols.

CAM was prepared *via* the conventional condensation reaction from commercially available cholic acid (CA) and ammonia by the mixed anhydride method at 243 K. Their inclusion compounds with three aliphatic secondary alcohols (**1–3**) were obtained by recrystallization from the corresponding racemic alcohols involving a small amount of ethanol. The resulting crystals had 1 : 1 stoichiometry of the host to guest by thermal gravimetric analysis. Their enclosed alcohols were recovered by micro-distillation. Enantiopurity of the alcohols was established by chiral HPLC analyses (Chiralcel OD–H or Chiralcel OJ–H column) using their phenyl carbamate derivatives.

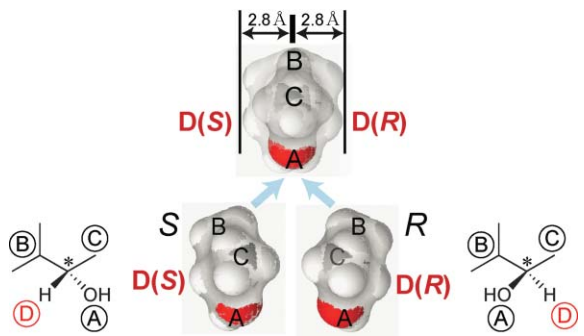

Fig. 1 Superposition of modeling structures for (*R*)- and (*S*)-3-methyl-2-butanol, one of the secondary aliphatic alcohols.

Department of Material and Life Science, Graduate School of Engineering, Osaka University 2-1 Yamadaoka, Suita, Osaka, 565-0871, Japan. E-mail: miyata@molrec.mls.eng.osaka-u.ac.jp; Fax: +81 6 6879 7406; Tel: +81 6 6879 7406

† Electronic supplementary information (ESI) available: Table S1: Hydrogen-bonding geometry for CAM·**2** and CAM·**3**. See DOI: 10.1039/b705822e

Table 1 shows the resulting enantiomeric excess (ee) values and the predominant configurations. The most remarkable feature is that (*S*)-**3** was obtained in more than 98% ee by the first recrystallization from the racemate, whereas **1** and **2** were obtained in less than 20% ee. To our knowledge, this is the first example of highly enantioselective enclathration of **3**. In addition, CAM·**3** crystals belong to space group $P2_12_12_1$, which is the first example among CAM crystals.

Crystallographic studies‡ brought us a profound insight for such an excellent enantioresolution. Fig. 2(a) and (b) illustrate molecular packing diagrams of the inclusion crystals of CAM with **2** and **3**, respectively. It can be seen that the host molecules construct common bilayer structures, and that the hydrophilic interface of the bilayers is similar in molecular arrangements (antiparallel), whereas the lipophilic one is different (antiparallel in **2** and parallel in **3**). Namely, addition of one methyl group to the isopropyl group induced the directional reversion of the bilayers in the lipophilic sides. Such a reversion in the lipophilic sides is very rare in case of bile acids and their derivatives.[6]

Furthermore, this "one methyl group effect" can be visualized in detail in the following way. Solvent accessible surfaces of the lipophilic sides are shown in Fig. 2(c) and (d), which involve stressed drawings of the guests as well as methyl groups at C18 and C19 of CAM (Scheme 1). It can be seen from comparison of these figures that (i) relative positions of the guests and the methyl groups are greatly different from each other, (ii) the methyl groups at C18 and C19 align with 2_1-axes perpendicular to each other, (iii) the host molecules form channel-like cavities along the 2_1-axes in **2**, whereas cage-like ones are formed in **3**, and (iv) the intermolecular distance between adjacent host molecules increases to 9.165 Å in **3** from 7.845 Å in **2**.

Table 1 Enantioresolution of aliphatic secondary alcohols by CAM

Alcohol	ee (%)	Predominant configuration
1[a]	19	*R*
2	19	*S*
3	98	*S*

[a] See ref. 5.

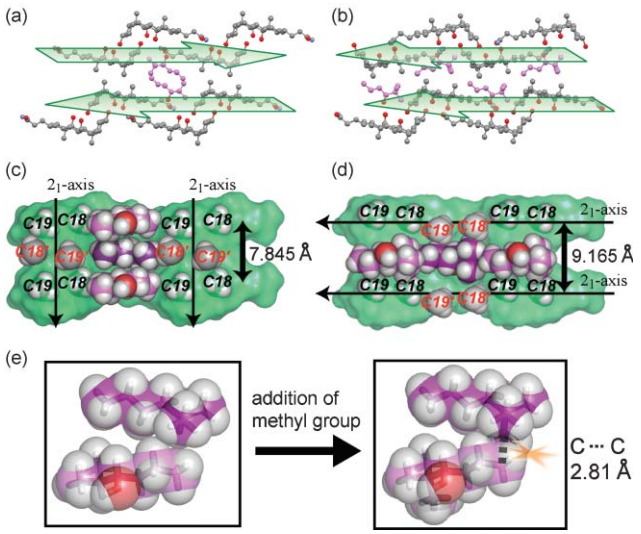

Fig. 2 Crystal structures of (a) CAM·**2** and (b) CAM·**3**. Hydrogen atoms are omitted for clarity. Host carbon, guest carbon, nitrogen and oxygen atoms are represented by gray, violet, blue and red, respectively. Host layered structures of (c) CAM·**2** and (d) CAM·**3** are drawn by solvent accessible surfaces in light green. C18 and C19 represent the methyl groups of CAM in the lower surface and C18′ and C19′ represent the methyl groups of CAM in the upper surface. (e) Hypothetical including guest **3** in the CAM·**2** host framework.

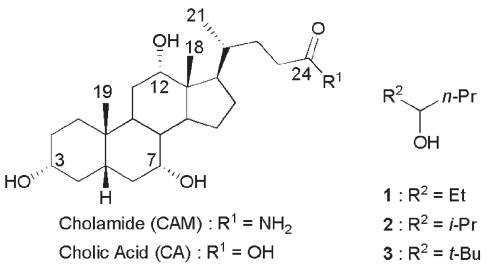

Scheme 1

These changes by the addition of one methyl group are reasonably explained on the basis of the following two simulations. One is that the replacement of the isopropyl group by *tert*-butyl group in the framework of CAM·**2** would result in steric repulsion between the guest molecules, as shown in Fig. 2(e). The other is a packing problem in the crystals. Our previous report clarified that the maximum packing coefficient of the CAM cavities for aliphatic alcohols is about 70%.[7] However, a hypothetical inclusion of **3** in the CAM·**2** framework gives an exceedingly large packing coefficient value (79%). Such a disadvantage is removed by the change of the stacking patterns of the bilayers. In this manner the slight difference between the guests **2** and **3** induces drastic differences between the assemblies CAM·**2** and CAM·**3**.

Next, we examine a relationship between the chiral recognition abilities and the cavity structures based on the four-location model.[8] As shown in Fig. 3, the model is based on the situation that a guest molecule goes inside a pocket of a host framework. In the case of secondary alcohols, A, B, C and D correspond to hydroxy group, large alkyl group, small alkyl group, and hydrogen, respectively. Even though three substituents (A, B and C) are fixed in the pocket, there are two possible locations for the fourth substituent D together with its neighboring stereogenic

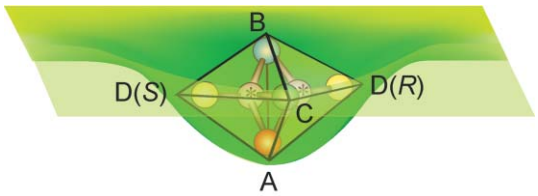

Fig. 3 The four-location model in a concave surface. Both enantiomers coexist in the pocket because of the disordered substituent D, even though three substituents around the stereogenic carbon (A, B and C) are fixed.

carbon. Therefore, we can discuss factors for selecting the fourth locations with respect to each substituent.

First, as for the substituent A, the hydrogen bonding networks are compared between CAM·**2** and CAM·**3**. As shown in Fig. 4(a), CAM·**2** has cyclic networks, which are bridged by OH(guest) with a sequence of NH(C24)···OH(guest)···O(C24). The hydrogen-bonding distances are 3.18 and 3.12 Å, respectively, indicating that the guest molecules are caught through loose hydrogen bonds. On the other hand, in the case of CAM·**3** (Fig. 4(b)), there exists smaller cyclic networks, which are bridged by OH(C12) and OH(guest) with a sequence of NH(C24)···OH(guest)··· OH(C12)···O(C24). The hydrogen-bonding distances are 2.879, 2.707 and 2.731 Å, respectively, indicating the guest molecule is tightly caught with O(C12). Of note is that each hydrogen-bonding distance in CAM·**3** is less than 3 Å, and that the hydrogen-bonding distances between the host and guest in the case of CAM·**3** are shorter than those in CAM·**2**. These differences indicate that the guest molecules in CAM·**3** are accommodated in the hole more strongly than those in CAM·**2**.

Second, as for the substituents B and C, we observed environments around the guest alcohol through cross-sectional views. For example, Fig. 5(a) and (b) depict the views of the cavities sliced by the planes perpendicular to the 2_1 axis in CAM·**2** and parallel to the 2_1 axis in CAM·**3**, respectively. These views reveal locations of the two alkyl groups around the hydroxyl groups. The *tert*-butyl group or isopropyl group is enclosed in the larger spherical space, while the *n*-propyl group is enclosed in the smaller slender space. It is impossible to replace the two positions of these alkyl groups in the cavity. Therefore, three locations (A, B and C) around the stereogenic carbon of these guest alcohols are determined.

Finally, the fourth D corresponds to hydrogen together with stereogenic carbon in this case. The location of D may be generally selected by attractive or repulsive interactions among the D and the surrounding hosts. Such interactions may be based on linear

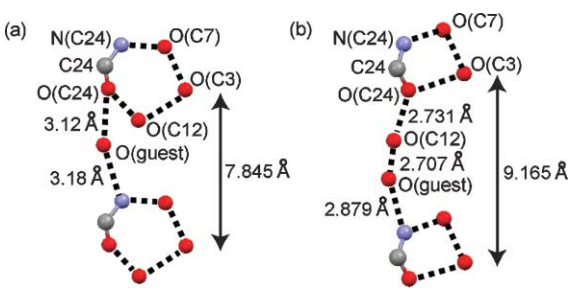

Fig. 4 Hydrogen bonding networks of (a) CAM·**2** and (b) CAM·**3**. O(C3), O(C7), O(C12), O(C24), O(guest) and N(C24) correspond to O1, O2, O3, O4, O5 and N1 in their CIFs, respectively. Detailed hydrogen bonding geometries are shown in ESI.†

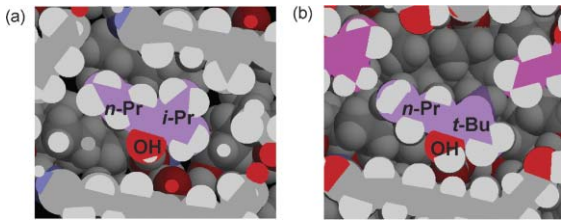

Fig. 5 The sectional views of the cavity sliced by the planes perpendicular to the channel (a) in CAM·**2** and (b) in CAM·**3**.

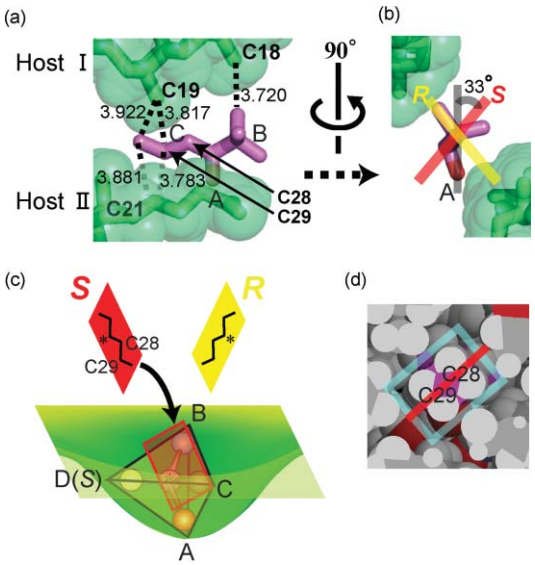

Fig. 6 (a) The van der Waals contact between the guest **3** and parts of the surrounding host molecules (hosts I and II). (b) Black, red and yellow lines represent a plane formed by three points (A, B and C), a *trans* plane of the *S*-isomer and a hypothetical plane of the *R*-isomer, respectively. (c) Schematic drawing of inclusion of a single enantiomer in the host pocket. (d) The sectional views of the cavity sliced by the planes perpendicular to the direction of the *trans* chain. The red line represents the *trans* plane.

weak bonds such as weak hydrogen bonds as well as spreading bonds such as van der Waals forces. The former interactions such as CH/O are not observed in the crystal structure of CAM inclusion compounds, and we focused on a van der Waals packing between the bilayers.

Electron density maps of crystal structures of CAM·**1** and CAM·**2** show that the guest molecules disorder around their stereogenic carbon. This indicates that these host frameworks have space to include both enantiomers of **1** or **2**. On the other hand, there is no space to include both enantiomers in CAM·**3** host framework. Fig. 6(a) and (b) show van der Waals contacts between the guest molecule **3** and parts of the surrounding host molecules. It can be seen that the methyl and methylene groups of the guest effectively contact the hosts at the 18- and 19-positions of the upper host I and at the 21-position of the lower host II, where the distances between the carbon atoms are about 3.8 Å. Furthermore, the guest molecule has a *trans* zigzag chain which is expressed as a plane involving stereogenic carbon and its neighboring carbons (red board in Fig. 6(b) and (c)). Fig. 6(d) shows that the plane is sandwiched between the plane of the host. The insertion of the enantiomeric plane (yellow board in Fig. 6(b) and (c)) would result in repulsion against the host molecules, explaining the efficient enantioselectivity.

In summary, the successful enantioresolution of racemic alkyl alcohols was achieved by the one methyl group effect on the reversion of the molecular arrangements. Furthermore, the chiral recognition is attributed to the selection of enantiomorphic faces involving stereogenic carbon and its two neighboring carbons on the basis of the strategy derived from the four-location model. We will now extensively investigate chiral recognition of other steroidal inclusion compounds.

K. A. expresses his special thanks to the Center of Excellence (21COE) program. This work was supported by a Grant-in-Aid for Scientific Research from the Ministry of Education, Culture, Sports, Science, and Technology, Japan.

Notes and references

‡ X-Ray crystal data of CAM·**2**, CAM·**3** were collected on a Rigaku RAXIS-RAPID Imaging Plate diffractometer at 98 and 93 K. *Crystal data*: CAM·**2**: $C_{31}H_{57}NO_5$, M = 523.79, monoclinic, space group $P2_1$, a = 12.1773(4), b = 7.8453(3), c = 16.2028(5) Å, β = 107.044(2)°, V = 1479.94(9) Å^3, Z = 2, μ(Cu-Kα) = 0.612 mm^{-1}, size 0.50 × 0.10 × 0.10 mm. 9181 total reflections, 2829 independent, 1355 observed. 321 parameters, R_1 [$I > 2\sigma(I)$] = 0.169. Guest molecules are disordered between *R* and *S* enantiomers. Only the predominant *S* enantiomer is shown in Fig. 2, 4 and 5; CAM·**3**: ($C_{32}H_{59}NO_5$), M = 537.82, orthorhombic, space group $P2_12_12_1$, a = 9.165(2), b = 16.668(3), c = 20.548(4) Å, V = 3138.9(10) Å^3, Z = 4, μ(Cu-Kα) = 0.588 mm^{-1}, size 0.20 × 0.20 × 0.20 mm. 28162 total reflections, 3220 independent, 1474 observed. 343 parameters, R_1 [$I > 2\sigma(I)$] = 0.049. CCDC 644113 and 644114. For crystallographic data in CIF or other electronic format see DOI: 10.1039/b705822e

1 Z. Urbanczyk-Lipkowska and F. Toda, *Perspectives in Supramolecular Chemistry (Separations and Reactions in Organic Supramolecular Chemistry)*, ed. F. Toda and R. Bishop, John Wiley & Sons, Chichester, UK, 2004, vol. 8, pp. 1–31.
2 (*a*) K. Tanaka, S. Honke, Z. Urbanczyk-Lipkowska and F. Toda, *Eur. J. Org. Chem.*, 2000, 3171; (*b*) K. Kodama, Y. Kobayashi and K. Saigo, *Chem. Eur. J.*, 2007, **13**, 2144; (*c*) O. Bortolini, G. Fantin, M. Fogagnolo, A. Medici and P. Pedrini, *Chem. Commun.*, 2000, 365; (*d*) M. Akazome, A. Hirabayashi, K. Takaoka, S. Nomura and K. Ogura, *Tetrahedron*, 2005, **61**, 1107; (*e*) F. Toda and K. Tanaka, *Chem. Lett.*, 1985, **14**, 885; (*f*) M. Miyata, M. Shibakami and K. Takemoto, *J. Chem. Soc., Chem. Commun.*, 1988, 655; (*g*) F. Toda, K. Tanaka, T. Omata, K. Nakamura and T. Oshima, *J. Am. Chem. Soc.*, 1983, **105**, 5151.
3 (*a*) C. Kassai, Z. Juvancz, J. Balint, E. Fogassy and D. Kozma, *Tetrahedron*, 2000, **56**, 8355; (*b*) R.-G. Xiong, X.-Z. You, B. F. Abrahams, Z. Xue and C.-M. Che, *Angew. Chem., Int. Ed.*, 2001, **40**, 4422; (*c*) Y. Imai, T. Sato and R. Kuroda, *Chem. Commun.*, 2005, 3289; (*d*) Y.-M. Song, T. Zhou, X.-S. Wang, X.-N. Li and R.-G. Xiong, *Cryst. Growth Des.*, 2006, **6**, 14.
4 K. Kato, K. Aburaya, Y. Miyake, K. Sada, N. Tohnai and M. Miyata, *Chem. Commun.*, 2003, 2872.
5 K. Sada, T. Kondo and M. Miyata, *Tetrahedron: Asymmetry*, 1995, **6**, 2655.
6 (*a*) N. Yoswathananont, M. Miyata, K. Nakano and K. Sada, in ref. 1, pp. 87–122; (*b*) M. Miyata, K. Sada and N. Yoswathananont, *Encyclopedia of Supramolecular Chemistry*, ed. J. L. Atwood and J. W. Steed, Marcel Dekker, New York, 2004, pp. 441–451; (*c*) M. Miyata and K. Sada, *Comprehensive Supramolecular Chemistry, Solid-State Supramolecular Chemistry: Crystal Engineering*, ed. D. D. MacNicol, F. Toda and R. Bishop, Pergamon, Oxford, 1996, vol. 6, pp. 147–176.
7 N. Yoswathananont, K. Sada, K. Nakano, K. Aburaya, M. Shigesato, Y. Hishikawa, K. Tani, N. Tohnai and M. Miyata, *Eur. J. Org. Chem.*, 2005, 5330.
8 (*a*) P. E. Wilcox, C. Heidelberger and V. R. Potter, *J. Am. Chem. Soc.*, 1950, **72**, 5019; (*b*) S. Topiol and M. Sabio, *J. Am. Chem. Soc.*, 1989, **111**, 4109; (*c*) A. D. Mesecar and D. E. Koshland, Jr., *Nature*, 2000, **403**, 614; (*d*) R. Bentley, *Arch. Biochem. Biophys.*, 2003, **414**, 1; (*e*) A. Mezzetti, J. D. Schrag, C. S. Cheong and R. J. Kazlauskas, *Chem. Biol.*, 2005, **12**, 427.